# Learned Mixed Material Models for Efficient Clustering Based Dual-Energy CT Image Decomposition

Zhipeng Li[1], Saiprasad Ravishankar[2,3], Yong Long[1], Jeffrey A. Fessler[2]

[1]University of Michigan - Shanghai Jiao Tong University Joint Institute,
Shanghai Jiao Tong University, Shanghai, China
[2]Department of Electrical Engineering and Computer Science,
University of Michigan, Ann Arbor, MI, USA
[3]Theoretical Division, Los Alamos National Laboratory, NM, USA

November 28, 2018


# Outline of Talk

1. Introduction
2. Dual-Energy CT (DECT) Image Decomposition Problem Formulation
3. DECT-MULTRA Algorithm Using Mixed Union of Learned TRAnsforms
4. Experiments and Results
5. Conclusions

# Motivation

- Dual-Energy CT (DECT)
  - Increasingly used in many clinical applications and industrial applications.
  - Enables characterizing concentration of constituent materials in scanned objects, known as material decomposition.[1]

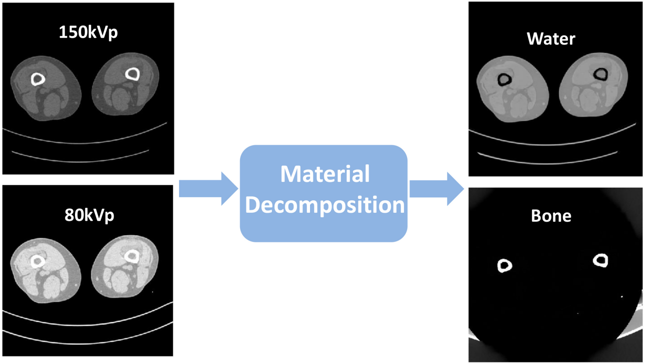


[1] [Mendonca et al., IEEE T-MI, 2014]

# Focus of This Talk: Image–Domain Decomposition

- Produces basis material images directly from attenuation images at low and high energies.
  - highly efficient – no forward or backprojections.
  - efficacy may be limited due to sensitivity to noise and artifacts.
- Conventional Image-Domain Decomposition (without regularization)
  - Direct matrix inversion decomposition[2]
- Regularized (model-based) Decomposition
  - Statistical decomposition model + Prior information of the material densities.
  - Improves image quality and decomposition accuracy.

[2] [Niu et al., MP, 2014]

# Regularization Approches for DECT

- Non-adaptive regularization
  - Material-wise Edge-Preserving (EP)[3]
    - suppresses noise while retaining boundary sharpness
    - simple prior
- Learning-based (sparsity) regularization
  - Dictionary Learning
    - has shown promise for DECT[4]
    - non-convex and NP-hard sparse coding
  - Sparsifying Transform (ST) Learning
    - DECT-ST[5]: recently proposed material-wise ST method
    - DECT-MULTRA: proposed approach based on a mixed union of learned transforms model which captures both common properties and cross-dependencies of basis materials

[3] [Xue et al., MP, 2017]
[4] [Li et al., ISBI, 2012]
[5] [Li et al., ISBI, 2018]

# Regularization Approches for DECT

- Non-adaptive regularization
  - Material-wise Edge-Preserving (EP)[3]
    - suppresses noise while retaining boundary sharpness
    - simple prior
- Learning-based (sparsity) regularization
  - Dictionary Learning
    - has shown promise for DECT[4]
    - non-convex and NP-hard sparse coding
  - Sparsifying Transform (ST) Learning
    - DECT-ST[5]: recently proposed material-wise ST method
    - DECT-MULTRA: proposed approach based on a mixed union of learned transforms model which captures both common properties and cross-dependencies of basis materials

[3] [Xue et al., MP, 2017]
[4] [Li et al., ISBI, 2012]
[5] [Li et al., ISBI, 2018]

# Outline


1. Introduction
2. Dual-Energy CT (DECT) Image Decomposition Problem Formulation
3. DECT-MULTRA Algorithm Using Mixed Union of Learned TRAnsforms
4. Experiments and Results
5. Conclusions

# Mixed Sparsifying Transform Model: Common and Cross Material

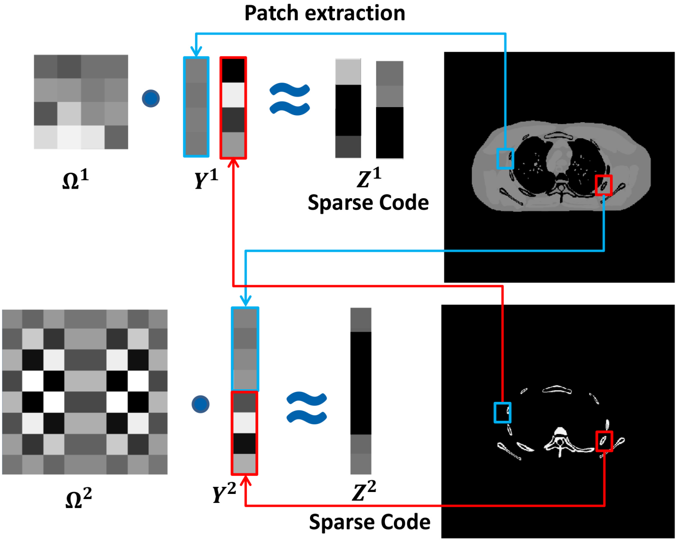

# Mixed Union of Learned TRAnsforms (MULTRA): Training

$$\min_{\{\mathbf{\Omega}^r_{k_r}, C^r_{k_r}, \mathbf{Z}^r_{i_r}\}} \sum_{k_r=1}^{K'_r} \sum_{i_r \in C^r_{k_r}} \left\{ \|\mathbf{\Omega}^r_{k_r} \mathbf{Y}^r_{i_r} - \mathbf{Z}^r_{i_r}\|_2^2 + \eta^2 \|\mathbf{Z}^r_{i_r}\|_0 \right\}$$

$$\text{s.t.} \quad {\mathbf{\Omega}^r_{k_r}}^T \mathbf{\Omega}^r_{k_r} = \mathbf{I}, \; 1 \le k_r \le K'_r, \qquad \text{(P0)}$$

- We learn two sets of transforms, one for common-material ($r = 1$) patches and one for cross-material ($r = 2$) patches. (P0) is solved for each $r$.
- $\{\mathbf{\Omega}^1_{k_r}\}$: set of $m \times m$ transforms for $r = 1$. $\{\mathbf{\Omega}^2_{k_r}\}$: $2m \times 2m$ transforms.
- $\mathbf{Y}^r_{i_r}$: a vectorized training patch, $\mathbf{Z}^r_{i_r}$: sparse code.
- Each patch is grouped with one transform. $C^r_{k_r}$: set with indices of patches belonging to the $k_r^{\text{th}}$ group/cluster in the $r$th model.
- An efficient alternating algorithm is used for joint clustering and learning[6].

[6] [Ravishankar & Bresler, IEEE TCI, 2016]

# MULTRA Model Notation during DECT Decomposition

Learned common-material transforms are used to form the blocks of the block-diagonal $\{\boldsymbol{\Omega}_{k_1}^1\}$. Cross-material transforms remain unchanged.

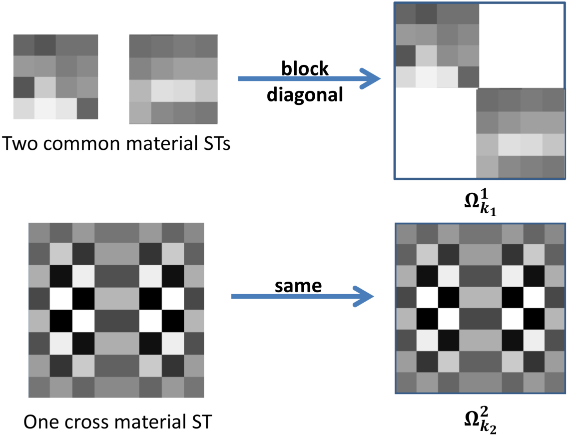

# DECT-MULTRA Formulation: Joint Clustering and Decomposition

$$\min_{\substack{\mathbf{x}\in\mathbb{R}^{2N_p},\\ \{\mathbf{z}_j, C^r_{k_r}\}}} \frac{1}{2}\|\mathbf{y}-\mathbf{A}\mathbf{x}\|^2_{\mathbf{W}} + \sum_{r=1}^{2}\sum_{k_r=1}^{K_r}\sum_{j\in C^r_{k_r}} \beta\Big\{\left\|\mathbf{\Omega}^r_{k_r}\mathbf{P}_j\mathbf{x}-\mathbf{z}_j\right\|_2^2 + \gamma_r^2\left\|\mathbf{z}_j\right\|_0\Big\} \quad \text{(P1)}$$

- $\mathbf{y} = (\mathbf{y}_H^T, \mathbf{y}_L^T)^T \in \mathbb{R}^{2N_p}$: attenuation maps at high and low energy.
- $\mathbf{x} = (\mathbf{x}_1^T, \mathbf{x}_2^T)^T \in \mathbb{R}^{2N_p}$: unknown material density images.
- $\mathbf{A} = \mathbf{A}_0 \otimes \mathbf{I}_{N_p}$: matrix of mass attenuation coefficients,
$$\mathbf{A}_0 = \begin{pmatrix} \varphi_{1H} & \varphi_{2H} \\ \varphi_{1L} & \varphi_{2L} \end{pmatrix}.$$
- $\mathbf{W} = \mathbf{W}_j \otimes \mathbf{I}_{N_p}$: weight matrix with $\mathbf{W}_j$ being the inverse noise covariance matrix.
- $\mathbf{P}_j \in \mathbb{R}^{2m\times 2N_p}$: extracts the $j$th 3D patch of $\mathbf{x}$ as a vector $\mathbf{P}_j\mathbf{x}$.
- $\mathbf{z}_j \in \mathbb{R}^{2m}$: transform sparse code of $\mathbf{P}_j\mathbf{x}$.

# Outline


1. Introduction
2. Dual-Energy CT (DECT) Image Decomposition Problem Formulation
3. DECT-MULTRA Algorithm Using Mixed Union of Learned TRAnsforms
4. Experiments and Results
5. Conclusions

# DECT-MULTRA Methodology

$$\min_{\substack{\mathbf{x}\in\mathbb{R}^{2N_p},\\ \{\mathbf{z}_j, C^r_{k_r}\}}} \frac{1}{2}\|\mathbf{y}-\mathbf{A}\mathbf{x}\|^2_{\mathbf{W}} + \sum_{r=1}^{2}\sum_{k_r=1}^{K_r}\sum_{j\in C^r_{k_r}} \beta\left\{ \left\|\mathbf{\Omega}^r_{k_r}\mathbf{P}_j\mathbf{x}-\mathbf{z}_j\right\|_2^2 + \gamma_r^2\left\|\mathbf{z}_j\right\|_0 \right\}, \quad \text{(P1)}$$

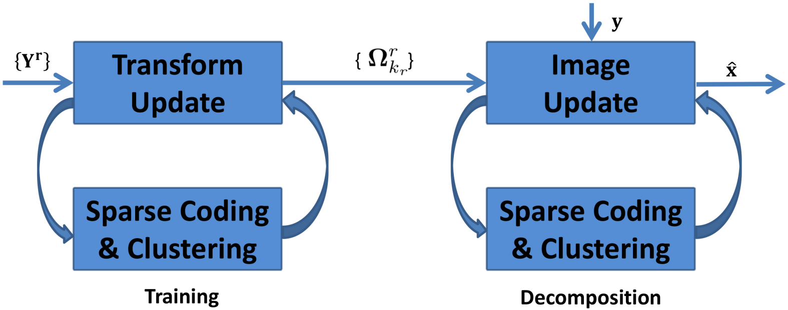


- Each step of the alternating algorithms has a closed-form update.

# Decomposition: Sparse Coding and Clustering Step

$$\min_{\{\mathbf{z}_j, C_{k_r}^r\}} \sum_{r=1}^{2} \sum_{k_r=1}^{K_r} \sum_{j \in C_{k_r}^r} \left\{ \left\| \mathbf{\Omega}_{k_r}^r \mathbf{P}_j \mathbf{x} - \mathbf{z}_j \right\|_2^2 + \gamma_r^2 \left\| \mathbf{z}_j \right\|_0 \right\}. \quad (1)$$

- Hard-thresholding operator $H_\gamma(\cdot)$ sets entries with mag. $< \gamma$ to 0.
- For each patch, the optimal cluster assignment is

$$(\hat{r}_j, \hat{k}_j) = \underset{\substack{1 \leq k_r \leq K_r \\ 1 \leq r \leq 2}}{\arg\min} \left\{ \left\| \mathbf{\Omega}_{k_r}^r \mathbf{P}_j \mathbf{x} - H_{\gamma_r}(\mathbf{\Omega}_{k_r}^r \mathbf{P}_j \mathbf{x}) \right\|_2^2 + \gamma_r^2 \left\| H_{\gamma_r}(\mathbf{\Omega}_{k_r}^r \mathbf{P}_j \mathbf{x}) \right\|_0 \right\}. \quad (2)$$

- The optimal sparse codes are then obtained as

$$\hat{\mathbf{z}}_j = H_{\gamma_{\hat{r}_j}}(\mathbf{\Omega}_{\hat{k}_j}^{\hat{r}_j} \mathbf{P}_j \mathbf{x}) \quad \forall j. \quad (3)$$

# Decomposition: Material Image Update Step

$$\min_{\mathbf{x}\in\mathbb{R}^{2N_p}} \frac{1}{2}\|\mathbf{y}-\mathbf{A}\mathbf{x}\|_{\mathbf{W}}^2 + \sum_{r=1}^{2}\sum_{k_r=1}^{K_r}\sum_{j\in C_{k_r}^r} \beta\left\|\mathbf{\Omega}_{k_r}^r \mathbf{P}_j\mathbf{x} - \mathbf{z}_j\right\|_2^2. \quad (4)$$

- Since $\mathbf{A}$ and $\mathbf{W}$ are block-diagonal and the transforms $\mathbf{\Omega}_{k_r}^r$ are unitary, the optimum solution is obtained pixel-wise as

$$\hat{\mathbf{x}}_j = \mathbf{B}_j^{-1}(\mathbf{A}_0^T\mathbf{W}_j\mathbf{y}_j + 2\beta\mathbf{M}_j\sum_{r=1}^{2}\sum_{k_r=1}^{K_r}\sum_{j\in C_{k_r}^r}\mathbf{P}_j^T\mathbf{\Omega}_{k_r}^{r\,T}\mathbf{z}_j). \quad (5)$$

  - $\hat{\mathbf{x}}_j$ is a vector with densities of materials at the $j$th pixel.
  - $\mathbf{M}_j$ is a matrix that extracts components corresponding to the $j$th pixel.
  - Update involves inverting the $2\times 2$ matrix $\mathbf{B}_j = \mathbf{A}_0^T\mathbf{W}_j\mathbf{A}_0 + 2\beta m\mathbf{I}_2 \ \forall\ j$.

# Outline


1. Introduction
2. Dual-Energy CT (DECT) Image Decomposition Problem Formulation
3. DECT-MULTRA Algorithm Using Mixed Union of Learned TRAnsforms
4. Experiments and Results
5. Conclusions

# Training MULTRA with XCAT phantom[7]

**Common-Material Union of Transforms ($K_1' = 15$)**

- Learned from $8 \times 8$ patches extracted from five slices of water images and five slices of bone images of the XCAT phantom.

**Cross-Material Union of Transforms ($K_2' = 10$)**

- Learned from $8 \times 8 \times 2$ patches extracted from five slices of cross-material images (water and bone images stacked together to form 3D volumns).

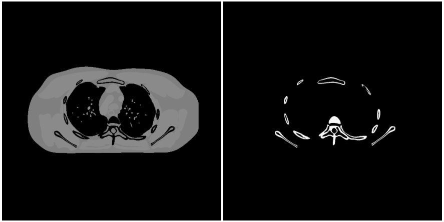

An example of training slices.

[7] [Segars et al., MP, 2008]

# DECT Simulation Setup

- Measurements simulation:
  - Image size: $1024 \times 1024$
  - Pixel size: $0.49 \times 0.49$ mm$^2$
  - Poly-energetic source: 80kVp and 140kVp with $1.86 \times 10^5$ and $1 \times 10^6$ incident photons per ray.
  - Sinogram sizes: $888 \times 984$
  - Reconstruct attenuation images via FBP.
- Decomposition:
  - Test images: 3 different slices of the XCAT phantom.
  - Image size: $512 \times 512$
  - Pixel size: $0.98 \times 0.98$ mm$^2$
  - Optimal parameters chosen to achieve the best image quality and decompositon accuracy.

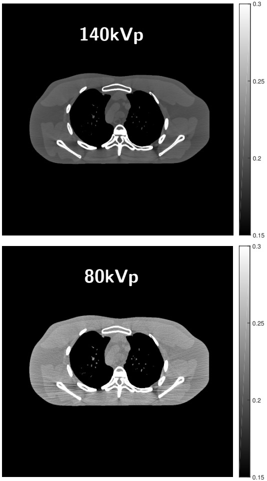


*High and low energy atten. images for a test slice*

# Material Image Root Mean Square Error Comparisons

Table: RMSE in $10^{-3}$ g/cm$^3$ of decompositions.

| Method | | Direct Inversion | DECT-EP | DECT-ST | DECT-MULTRA |
|---|---|---|---|---|---|
| Slice 61 | Water | 72.8 | 60.9 | 51.3 | **42.8** |
| | Bone | 68.4 | 60.2 | 51.6 | **43.9** |
| Slice 77 | Water | 92.4 | 65.9 | 55.6 | **38.7** |
| | Bone | 89.0 | 72.2 | 61.8 | **49.8** |
| Slice 150 | Water | 116.7 | 69.1 | 61.7 | **38.6** |
| | Bone | 110.8 | 76.7 | 67.0 | **50.8** |

- Direct Inversion obtains material images directly without regularization.
- DECT-MULTRA improves the RMSE achieved by nonadaptive DECT-EP.
- DECT-MULTRA with unions of transforms outperforms DECT-ST that uses learned square transforms for water and bone patches, respectively.

# Visual Results

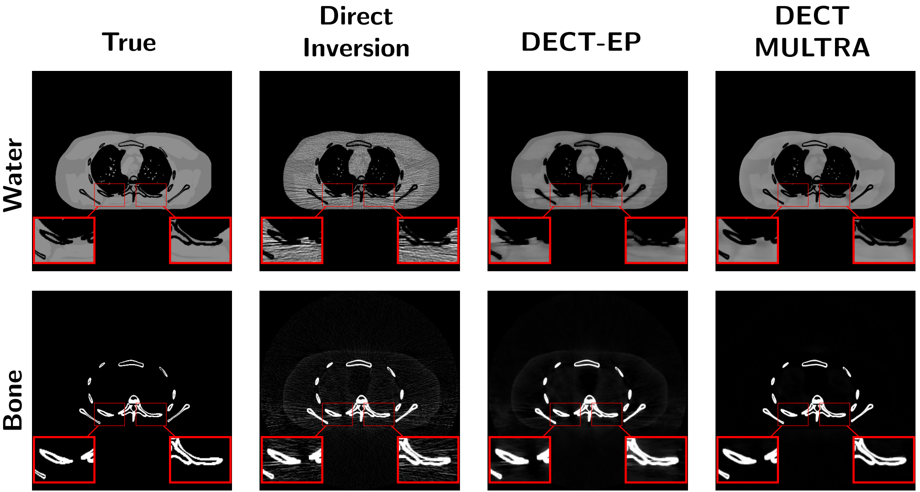


Water and bone image display windows: [0.6 1.4] $g/cm^3$ and [0 0.8] $g/cm^3$, respectively.

# Visual Results

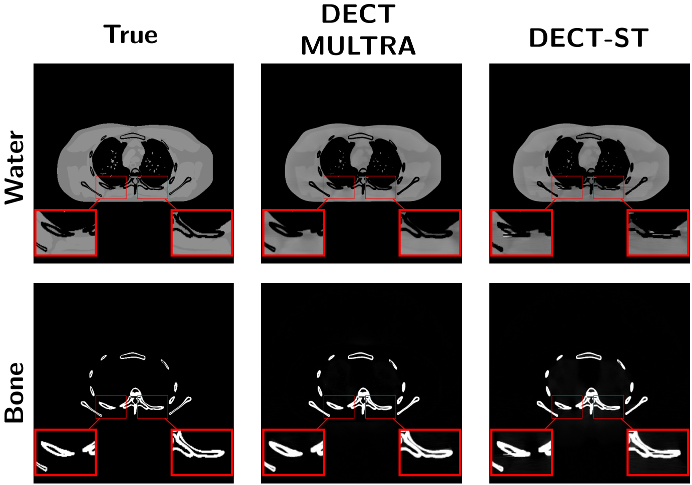


- DECT-MULTRA outperforms DECT-ST by reducing artifacts and improving edge details.

# An Example of Cross-Material Clustering Results

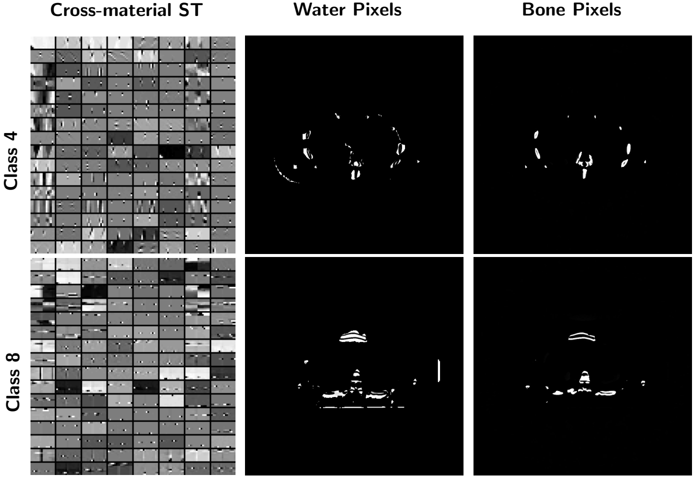


Water and bone display windows: $[0.4\ 1]\,\mathrm{g/cm^3}$ and $[0\ 0.8]\,\mathrm{g/cm^3}$.

- Pixels are clustered by majority vote among the patches overlapping them.

# Outline

1 Introduction

2 Dual-Energy CT (DECT) Image Decomposition Problem Formulation

3 DECT-MULTRA Algorithm Using Mixed Union of Learned TRAnsforms

4 Experiments and Results

5 Conclusions

- **Conclusions**
  - We proposed DECT-MULTRA combining PWLS estimation with regularization based on a mixed union of learned unitary transforms.
  - Proposed approach exploits both the common properties among material images and their cross-dependencies.
  - DECT-MULTRA provided better material image quality and decomposition accuracy than the recent DECT-ST and nonadaptive DECT-EP methods.
- **Future Work**
  - Investigate more general multi-material (with several materials) decompositions with DECT-MULTRA.

**Thank You! Questions??**